

Raman scattering from a superconductivity-induced bound state in MgB_2

R. Zeyher

Max-Planck-Institut für Festkörperforschung,
Heisenbergstr.1, 70569 Stuttgart, Germany
(November 3, 2018)

It is shown that the sharp peak in the E_{2g} Raman spectrum of superconducting MgB_2 is due to a bound state caused by the electron-phonon coupling. Our theory explains why this peak appears only in the spectra with E_{2g} symmetry and only in the σ but not π bands. The properties of the bound state and the Raman spectrum are investigated, also in the presence of impurity scattering.

PACS numbers:74.70.Ad, 74.25.Nf, 74.25.Kc

Electronic Raman scattering in superconductors probes the density and, to some extent, the momentum dependence of quasi-particle excitations across the gap. As a result the spectra are usually dominated by broad pair breaking peaks reflecting the magnitude and anisotropy of the gap as well as scattering processes of the quasi-particles. Experimental spectra in the two-gap superconductor MgB_2 show the typical features of a dirty s-wave superconductor [1,2]. A new and surprising feature in the E_{2g} spectrum is a sharp peak near the larger of the two gaps which in our opinion cannot be explained as a pair breaking peak because of the large impurity scattering rate of quasi-particles in the present MgB_2 samples. Below we will argue that this peak is the analogue of the magnetic resonance peak observed in high- T_c cuprates [3] where the electron-phonon interaction takes over the role of the Heisenberg interaction and strongly scatters the excitations across the gap.

Neglecting the momenta of the incident and scattered photons the differential Raman cross section can be written as

$$\frac{d^2 R}{d\omega d\Omega} = -\frac{e^4}{\pi c^4} (1 + n(\omega)) \chi''(\omega). \quad (1)$$

e is the charge of an electron, $n(\omega)$ the Bose distribution function, ω the difference in frequency between incident and scattered light, and χ'' the imaginary part of a retarded Green's function χ at zero momentum. The corresponding Matsubara function is

$$\chi(i\omega_n) = -\int_0^\beta d\tau e^{i\omega_n \tau} \langle T_\tau \rho(\tau) \rho(0) \rangle, \quad (2)$$

where β is the inverse temperature $1/T$, $\omega_n = 2n\pi T$ are bosonic Matsubara frequencies, T_τ the time ordering operator, and ρ an effective density operator with momentum zero. In the following we will be interested in spectra related to the E_{2g} symmetry of D_{6h} , the point group of MgB_2 . ρ has then the form

$$\rho = \sum_{\mathbf{k}\sigma n} \gamma_n(\mathbf{k}) c_{\sigma n}^\dagger(\mathbf{k}) c_{\sigma n}(\mathbf{k}) + R(b + b^\dagger), \quad (3)$$

$$\gamma_n(\mathbf{k}) = \left(\frac{\partial^2 \epsilon_n(\mathbf{k})}{\partial k_x^2} - \frac{\partial^2 \epsilon_n(\mathbf{k})}{\partial k_y^2} \right). \quad (4)$$

$c_{\sigma n}^\dagger(\mathbf{k})$ and $c_{\sigma n}(\mathbf{k})$ are creation and annihilation operators for electrons with momentum \mathbf{k} , spin direction σ , band label n , and energy $\epsilon_n(\mathbf{k})$. MgB_2 has only one Raman-active $\mathbf{q} = 0$ phonon, and this phonon has E_{2g} symmetry. Its frequency is denoted by Ω , its creation and annihilation operators by b^\dagger and b , respectively, and the corresponding element of the phononic Raman tensor by R . Without loss of generality we assume that this phonon transforms as the first basis vector of the two-dimensional E_{2g} representation in accordance with Eq.(4).

For the evaluation of χ we use the Hamiltonian $H = H_0 + H'$ with

$$H_0 = \sum_{\mathbf{k}\sigma n} \epsilon_n(\mathbf{k}) c_{\sigma n}^\dagger(\mathbf{k}) c_{\sigma n}(\mathbf{k}) + \sum_{\mathbf{q}j} \Omega_j(\mathbf{q}) (b_j^\dagger(\mathbf{q}) b_j(\mathbf{q}) + \frac{1}{2}) - \sum_n \left(\Delta_n c_{\uparrow n}^\dagger(\mathbf{k}) c_{\downarrow n}^\dagger(-\mathbf{k}) + h.c. \right), \quad (5)$$

$$H' = \sum_{\mathbf{k}\mathbf{q}n} g_{nj}(\mathbf{k}\mathbf{q}) c_{\sigma n}^\dagger(\mathbf{k} + \mathbf{q}) c_{\sigma n}(\mathbf{k}) (b_j(\mathbf{q}) + b_j^\dagger(-\mathbf{q})) + \sum_{\substack{\mathbf{k}\mathbf{q}\sigma \\ nn'}} V_{nn'}(\mathbf{k}\mathbf{q}) c_{\sigma n}^\dagger(\mathbf{k}) c_{\sigma n'}(\mathbf{q}). \quad (6)$$

Δ_n is the gap parameter for s-wave superconductivity in the band n , $\Omega_j(\mathbf{q})$ the frequency of a general phonon with momentum \mathbf{q} and branch label j , g the coupling constant for intraband electron-phonon scattering and V a random potential for intraband impurity scattering. Interband phonon scattering can be neglected in H' because only zero momentum transfers occur in the approximation used below.

In a first step we perform an infinite summation over bubble diagrams by introducing the irreducible Green's function $\tilde{\chi}$. $\tilde{\chi}$ contains all diagrams to χ which cannot be decomposed into two parts by cutting one phonon line. The average over impurities yields impurity lines with similar properties as phonon lines. However, bubble diagrams connected by impurity lines are not possible in this case so that the above definition of irreducibility is appropriate. Analytically, one obtains

$$\chi = \tilde{\chi}_{11} + (\tilde{\chi}_{12} + R)D(R + \tilde{\chi}_{21}), \quad (7)$$

$$D = D^{(0)} + D^{(0)}\tilde{\chi}_{22}D. \quad (8)$$

The omitted frequency and momentum arguments in the Green's functions in Eqs.(7) and (8) are $i\omega_n$ and 0, respectively. $\tilde{\chi}_{11}$ denotes the irreducible Green's function associated with the two vertices $\gamma_n(\mathbf{k})$. Similarly, the vertices in the functions $\tilde{\chi}_{12}$ and $\tilde{\chi}_{22}$ are $\gamma_n(\mathbf{k})$ and $g_n(\mathbf{k}0)$, and two times $g_n(\mathbf{k}0)$, respectively. The free phonon propagator $D^{(0)}$ is given by $-2\Omega/(\omega_n^2 + \Omega^2)$.

A sensible approximation for the evaluation of $\tilde{\chi}$ is the ladder approximation plus the corresponding self-energy corrections where the interaction lines are due to phonons or impurities. Only that part of the interaction can contribute in the ladder diagrams which transforms in the same way as the vertices γ and g . This means in our case that only the E_{2g} component of the phonon-mediated interaction, which usually is considered to be negligible in a s-wave superconductor, would enter. We therefore will evaluate $\tilde{\chi}$ only in the presence of random impurities using the Born approximation and the dirty limit for each band. Assuming that the vertices and the interaction can be evaluated right on the Fermi surface, expanding γ and g in terms of Fermi surface harmonics [4] of E_{2g} symmetry, $\Phi_L^{(n)}(\mathbf{k})$, normalized as in Eq.(1) of Ref. [4],

$$\gamma_n(\mathbf{k}) = \sum_L \alpha_{1L}^{(n)} \Phi_L^{(n)}(\mathbf{k}), \quad (9)$$

$$g_n(\mathbf{k}0) = \sum_L \alpha_{2L}^{(n)} \Phi_L^{(n)}(\mathbf{k}), \quad (10)$$

and assuming that the interaction is diagonal in L we obtain

$$\tilde{\chi}_{ij}(i\omega_n) = \sum_{Ln} \alpha_{iL}^{(n)} \alpha_{jL}^{(n)} N_F^{(n)} \tilde{\chi}(i\omega_n, \Delta_n, \tau_n^{-1}). \quad (11)$$

$N_F^{(n)}$ is the density of states at the Fermi surface for one spin direction due to the band n and $1/\tau_n$ an effective scattering rate. After an analytic continuation $i\omega_n \rightarrow \omega + i\eta$ the imaginary part of the Green's function $\tilde{\chi}$, which is independent of L , becomes [5]

$$\begin{aligned} \text{Im } \tilde{\chi}(\omega, \Delta, \tau^{-1}) = & -\frac{8\Delta\omega}{\omega + 2\Delta} \Theta(\omega - 2\Delta) \frac{\tau^{-1}}{\omega^2 + \tau^{-2}} \\ & \cdot \left(\frac{(\omega - 2\Delta)^2}{4\Delta\omega} E(\alpha) + \frac{\tau^{-2} + \omega^2 + 4\Delta\omega}{\tau^{-2} + \omega^2 + 2\Delta\omega} F(\alpha) \right. \\ & \left. + \frac{8\Delta^2\omega^2}{(\omega^2 + \tau^{-2})^2 - 4\Delta^2\omega^2} \Pi(N, \alpha) \right), \quad (12) \end{aligned}$$

with

$$\alpha = (\omega - 2\Delta)/(\omega + 2\Delta), \quad (13)$$

$$N = \frac{1 + \alpha^2\omega_1}{1 + \omega_1}, \quad (14)$$

$$\omega_1 = \tau^{-2}(1 - 4\Delta^2/(\omega^2 + \tau^{-2})) / (\omega - 2\Delta)^2. \quad (15)$$

Θ is the theta function and F , E , and Π are complete elliptical integrals of the first, second, and third kinds, respectively. The existence of only two gaps in the experimental spectra [1,2,6] as well as theoretical arguments [7] suggest that the dirty limit applies even within the two-band complex of σ and π bands (denoted by the index ρ in the following) and that the interband impurity scattering between σ and π bands is negligible. As a result Δ_n and τ_n^{-1} can be considered to be the same within the manifold of σ or π bands. Introducing then the effective couplings

$$\lambda_{ij}^{(\rho)} = \sum_{\substack{L \\ n \in \rho}} \alpha_{iL}^{(n)} \alpha_{jL}^{(n)} N_F^{(n)}, \quad (16)$$

we obtain

$$\tilde{\chi}_{ij}(\omega) = \sum_{\rho=\sigma,\pi} \lambda_{ij}^{(\rho)} \tilde{\chi}(\omega, \Delta_\rho, \tau_\rho^{-1}). \quad (17)$$

Choosing for the first function $\Phi_1^{(n)}(\mathbf{k})$ the properly normalized function $\sim \gamma_n(\mathbf{k})$, the summations over L collapse to one term $L = 1$ if either i or j is equal to 1. In the clean limit $1/\tau \rightarrow 0$ Eq.(12) reduces to the analytical formula Eq.(16) of Ref. [8].

Using the tight-binding fit to the band structure of Ref. [9], eV as energy and the lattice constant a as length units, we find $N_F^{(1)} = 0.049$, $N_F^{(2)} = 0.109$, $N_F^{(3)} = 0.101$, $N_F^{(4)} = 0.104$, where $n = 1, 2$ denote the light and heavy σ bands and $n = 3, 4$ the π bands. In the case of π bands we have scaled the published tight-binding parameters slightly in order to reproduce the correct densities. Furthermore, we obtain $\alpha_1^{(1)} = 0.101$, $\alpha_1^{(2)} = 0.261$, $\alpha_1^{(3)} = 2.531$, $\alpha_1^{(4)} = 2.376$, and thus $\lambda_{11}^{(\sigma)} = 0.008$, and $\lambda_{11}^{(\pi)} = 1.238$. The rather small values for $\alpha_1^{(1)}$, $\alpha_1^{(2)}$, and $\lambda_{11}^{(\sigma)}$ reflect the fact that the σ bands are rather isotropic in the ab-plane near their narrow cylindrical Fermi surfaces and thus cannot contribute much in the E_{2g} channel. As a consequence we may safely put $\lambda_{11}^{(\sigma)} = \lambda_{12}^{(\sigma)} = \lambda_{21}^{(\sigma)} = 0$. The σ contribution to $\tilde{\chi}$ arises then solely from the coupling of the phonon to the light and its spectral features are determined by the dimensionless electron-phonon coupling constant $\lambda = \frac{2}{\Omega} \lambda_{22}^{(\sigma)}$ and the scattering rate $1/\tau_\sigma$.

We will first consider the σ contribution to $\tilde{\chi}$ and drop the index σ everywhere in order to simplify the notation. Fig.1 shows the real (dashed lines) and imaginary (solid lines) part of $\tilde{\chi}$ for the gap $2\Delta = 110\text{cm}^{-1}$ and two scattering rates $1/\tau = 0$ and $1/\tau = 200\text{cm}^{-1}$. In the clean

case the imaginary part $\tilde{\chi}''$ exhibits a square root singularity if ω approaches 2Δ from above. Impurity scattering transforms this singularity into a step at 2Δ with height $2\pi\Delta\tau$, and produces for sufficiently strong scattering a very broad minimum near $1/\tau$. The real part $\tilde{\chi}'$ shows in the clean case a square root singularity below 2Δ and finite and positive values above 2Δ . Taking impurity scattering into account $\tilde{\chi}'$ becomes much more symmetric around 2Δ compared to the clean case,

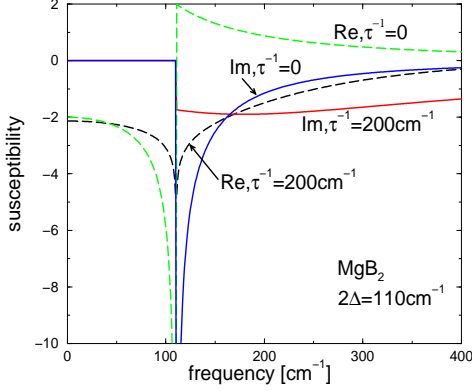


FIG. 1. Real (dashed lines) and imaginary (solid lines) part of the susceptibility $\tilde{\chi}$ for two impurity scattering rates τ^{-1} and parameters appropriate for MgB_2 .

exhibiting there a logarithmic singularity and negative values over a large region above 2Δ .

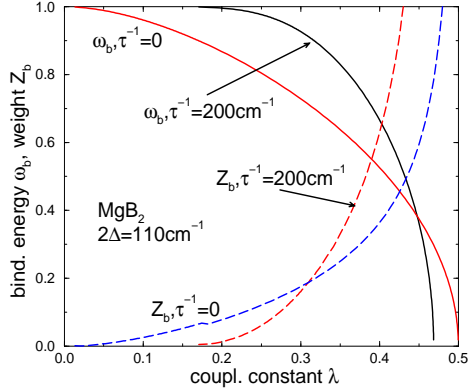


FIG. 2. Energy $\omega_b/2\Delta$ (solid curves) and spectral weight Z_b (dashed curves) of the bound state for two impurity scattering rates τ^{-1} as a function of the electron-phonon coupling constant λ .

The curves in Fig. 1 suggest that the phonon Green's function D will develop a bound state inside the gap [10], and that this will occur for all values for λ and $1/\tau$. The frequency of the bound state, ω_b , is determined by the vanishing of the denominator of D , i.e., by the equation,

$$\omega_b^2 = \Omega^2 + \Omega^2 \lambda \tilde{\chi}'(\omega_b, \Delta, 1/\tau). \quad (18)$$

Expanding the denominator of D around ω_b one finds for the spectral weight Z_b

$$Z_b = \frac{2\Omega}{2\omega_b - \lambda\Omega^2 \partial \tilde{\chi}'(\omega_b, \Delta, 1/\tau) / \partial \omega_b}. \quad (19)$$

Fig.2 shows ω_b and Z_b as a function of λ for the two scattering rates $1/\tau = 0$ and $1/\tau = 200\text{cm}^{-1}$. ω_b approaches zero at $\lambda_{CDW} = 0.50$ and 0.47 , respectively. This means that for $\lambda > \lambda_{CDW}$ the superconducting state is unstable against the formation of a charge density wave with E_{2g} symmetry. For $\lambda < \lambda_{CDW}$ ω_b and Z_b increase and decrease rapidly with decreasing λ approaching their limiting values 1 and 0 in an exponential (for $1/\tau \neq 0$) or powerlawlike (for $1/\tau = 0$) manner.

One peculiar feature of D is that any background imaginary part in its self-energy, for instance due to π electrons, will be diminished by the factor $1/Z_b$ near 2Δ . This means that the bound state will not be broadened

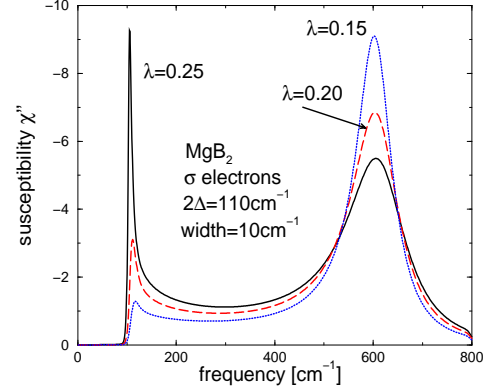


FIG. 3. Susceptibility χ'' of σ electrons at $T = 0$ for the scattering rate $\tau^{-1} = 200\text{cm}^{-1}$.

and disappear in χ'' for small λ 's, even in the presence of strong impurity scattering, but instead will sharpen and loose weight when ω_b approaches 1. To make the situation more realistic one should allow for broadening effects due to inhomogenities etc. which may be taken into account by folding $\tilde{\chi}'$ with a Gaussian with a width δ [2,5]. Fig.3 shows χ'' for three different λ and a width of $\delta = 10\text{cm}^{-1}$. The employed large scattering rate $\tau^{-1} = 200\text{cm}^{-1}$ has wiped out completely the usual pair breaking peak due to the square root divergence of χ'' at 2Δ . On the other hand, the electron-phonon coupling accumulates spectral weight near 2Δ and produces a pronounced bound state inside the gap at larger couplings.

Figs.2 and 3 allow to estimate a realistic value for λ . Identifying ω_b with the observed sharp peak in the E_{2g} spectrum we have $\omega_b = 104 \pm 1\text{cm}^{-1}$ whereas a recent tunneling experiment [6] gave for the gap $2\Delta =$

$114 \pm 6 \text{ cm}^{-1}$. This suggests that ω_b is different from 2Δ , i.e., the sharp peak should not be identified with the gap, and the ratio $\omega_b/2\Delta$ is 0.91 ± 0.06 . Fig.2 indicates then that λ must be smaller than 0.3. Comparing the intensities of the bound state and the phonon line in Fig.3 with the experimental curve [1] one finds that λ must be near the interval between 0.15 and 0.20. These values are substantially smaller than the value 0.38 obtained from band structure calculations [11].

Additional evidence for the importance of the electron-phonon coupling in the E_{2g} spectrum comes from the experimental result that the two A_{1g} and the E_{1g} spectra do not show any pronounced peak near 2Δ . We explain this by the fact that, according to group theory, MgB_2 has no $\mathbf{q} = 0$ phonons with such symmetries so that no

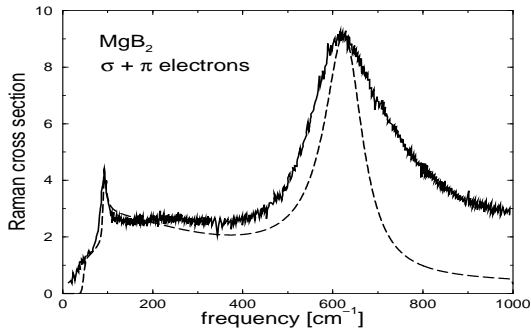


FIG. 4. Experimental (solid line) and theoretical (dashed line) E_{2g} Raman cross section.

bound states can be formed. Further support for the present theory comes from the absence of a peak near the gap of about 47 cm^{-1} in the π bands. LDA calculations show that the coupling of π electrons to the E_{2g} phonon is by a factor 3 or 4 smaller than for σ electrons [11]. We find that the bound state structure near the π gap is invisible for such a coupling which explains its absence in the experimental spectra. Using $\lambda_{12}^{(\pi)} = \lambda_{21}^{(\pi)} = 0$, $\lambda_{22}^{(\pi)}/\lambda_{22}^{(\sigma)} = 1/3$, $\lambda_{11}^{(\pi)}/R^2 = 1/400$, $\lambda = 0.16$, $\Omega = 620 \text{ cm}^{-1}$, $\delta = 5 \text{ cm}^{-1}$, a π gap of 43 cm^{-1} and a somewhat reduced σ gap of 96.5 cm^{-1} , accounting for the finite temperature of the experimental data, the resulting Raman cross section is shown as the dashed line in Fig.4, together with the experimental E_{2g} spectrum [1]. The dashed line reproduces well the main features of the experimental curve, especially at small frequencies. The quantitative discrepancy in the phonon

region suggests that only part of the phonon broadening is caused by the electron-phonon coupling and that anharmonicity and deviations from the assumed constant density of states may play a role. The theoretical superconductivity-induced hardening of the phonon frequency in Fig.4 is 5 cm^{-1} and thus somewhat smaller than the experimental value [1] of $7 - 10 \text{ cm}^{-1}$.

In conclusion, we have shown that the E_{2g} spectrum in superconducting MgB_2 can be understood as a superposition of a phonon line coupled strongly to σ electrons creating hereby a bound state in the gap, and a background due to rather uncorrelated π electrons. This means that MgB_2 is to our knowledge the first s-wave superconductor where a bound state in the superconducting gap due to residual interactions has been observed and identified. The obtained electron-phonon coupling constant $\lambda \sim 0.2$ for σ electrons is only half of the band structure value, a discrepancy, which presently is not well understood.

The author thanks O. Dolgov, J. Kortus and I. Mazin for useful discussions.

-
- [1] J.W. Quilty, S. Lee, A. Yamamoto, and S. Tajima, Phys. Rev. Lett. **88**, 87001 (2002)
 - [2] J.W. Quilty, S. Lee, S. Tajima, and A. Yamanaka, cond-mat/0206506
 - [3] See, for example, D.Z. Liu, Y. Zha, and K. Levin, Phys. Rev. Lett. **75**, 4130 (1995); I.I. Mazin and V.M. Yakovenko, Phys. Rev. Lett. **75**, 4134 (1995);
 - [4] P.A. Allen, Phys. Rev. B **13**, 1416 (1976)
 - [5] T.P. Devereaux, Phys. Rev. B **45**, 12965 (1992)
 - [6] R.S. Gonnelli, D. Daghero, G.A. Ummarino, V.A. Stepanov, J. Jun, S.M. Kazakov, and J. Karpinski, cond-mat/0209472
 - [7] I.I. Mazin, O.K. Andersen, O. Jepsen, O.V. Dolgov, J. Kortus, A.A. Golubov, A.B. Kuz'menko, and D. van der Marel, Phys. Rev. Lett. **89**, 107002 (2002)
 - [8] R. Zeyher and G. Zwircknagl, Sol. State Comm. **66**, 617 (1988)
 - [9] Y. Kong, O.V. Dolgov, O. Jepsen, and O.K. Andersen, Phys. Rev. B **64**, 20501 (2001)
 - [10] R. Zeyher and G. Zwircknagl, Z. Phys. B - Condensed Matter **78**, 175 (1990)
 - [11] A.Y. Liu, I.I. Mazin, and J. Kortus, Phys. Rev. Lett. **87**, 87005 (2001), and unpublished